

## Supporting Information :

# **Fluoro-electrochemical Microscopy reveals Group Specific Differential Susceptibility of Phytoplankton towards Oxidative Damage**

SI contents:

Section 1: Phytoplankton Structure

Section 2: Experimental

Section 3: Videos of the Fluoro-Electrochemical experiments

Section 4: Effect of Oxidative Potential on Phytoplankton  
Fluorescence

Section 5: Data analysis

Section 6: Chemical Effects on Phytoplankton Fluorescence

Section 7: Fluorescence response of *E.Huxleyi*

Section 8: Analytical Model for the Plankton Behaviour

## Section 1 : Phytoplankton Structure

This work studies a range of different phytoplankton species – a diatom (*Halamphora coffeaeformis*), a coccolithophore (*Emiliana huxleyi*), three fresh water green algae (*Chlorella singularis*, *Chlorella volutis* and *Stichococcus bacillaris*), a marine algae (*Nannochloropsis oceanica*) and a dinoflagellate (*Scrippsiella trochoidea*). All species are visible under light microscope and are approximately 2-10 µm in diameter apart from *S. trochoidea* which is significantly larger (25 µm). Under a light microscope they do not look dissimilar but species such as diatoms can be easily differentiated from others due to their unique shape and structure.

The diatom *H. coffeaeformis* is bilaterally symmetric in shape and consists of a porous silica frustule cell wall.<sup>1, 2</sup> Behind the cell wall lies the chlorophyll-a containing plastid (Mereschkowsky's type 2) - characteristic for the 'H' shape under fluorescence conditions.<sup>2</sup> *E. huxleyi* is a coccolithophore and appears spherical under the microscope. The life cycle of *E. huxleyi* contains three phases; the commonly known, non-motile and coccolith forming C-cell, the non-motile and 'naked' N-cell, and the motile scale-covered S-cell.<sup>3</sup> Both N-cells and S-cells may appear spontaneously in a culture of C-cells.<sup>4</sup> All the green algae under study and *N. oceanica* are spherical in shape with the exception that *S. bacillaris* is oval in shape. The cell wall composition of the algae is commonly in the form of cellulose.

## Section 2: Experimental

### *Chemicals*

All chemicals used were of analytical grade and were purchased from Sigma-Aldrich, with the exception of NaF which was purchased from Fluka. All chemicals were used without further purification. Aqueous solutions were made using ultrapure water (Millipore, resistivity 18.2 M $\Omega$  cm at 25 °C).

### *Phytoplankton culture*

The *Halamphora coffeaeformis* (diatom, CCAP 1001/2), *Stichococcus bacillaris* (freshwater algae, CCAP 379/1A), *Chlorella singularis* (freshwater algae, CCAP 211/119), *Chlorella volutis* (freshwater algae, CCAP 211/120) and *Nannochloropsis oceanica* (marine algae, CCAP 849/10) was obtained from Scottish Marine Institute, Scotland. The *Emiliania huxleyi* (coccolithophore, RCC 174) and *Scrippsiella trochoidea* (dinoflagellate, RCC 91) was sourced from the Roscoff Culture Collection (RCC), France. The phytoplankton were cultured under 16 hours of light and 8 hours of dark cycle at 22°C. The medium used here was largely following the recipe of f/2 medium from the Bigelow National Centre for Marine Algae and Microbiota (USA), but used synthetic ocean water instead of natural seawater. The synthetic ocean water was prepared following Morel *et al.*<sup>5</sup> The culture which the freshwater algae were grown in (3N-BBM+V) were exchanged with f/2 medium prior to the electrochemical experiments.

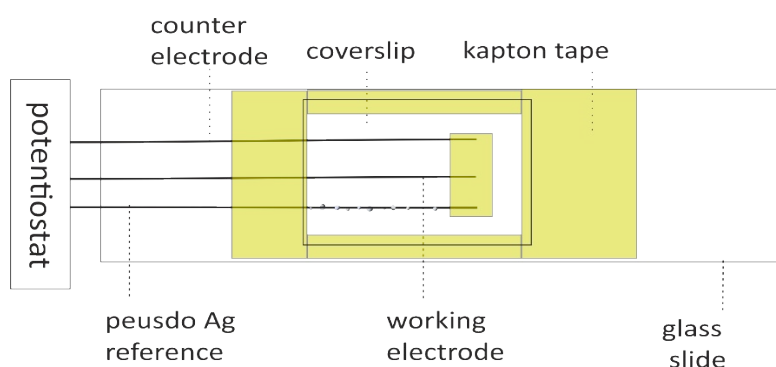
### *Microscope and Image Analysis*

The fluorescence excitation light source was provided by a LQ-HXP 120 V lamp. Optical measurements were made on a Zeiss Axio Examiner, A1 Epifluorescence microscope (Carl Zeiss Ltd., Cambridge U.K.) using a 20 $\times$  air objective (NA = 0.5, EC Plan-Neofluar) and 40 $\times$  oil immersion objective (Plan-Apochromat 40 $\times$ /1.3 Iris (UV)VIS-IR). The excitation filter was purchased from

Thorlab (FITC  $475 \pm 35\text{nm}$ ); the dichromic mirror and emission filter were from Zeiss filter set 15 which transmit emission wavelengths above 590nm. The video acquisition was provided by a Hamamatsu ORCA-Flash 4.0 digital CMOS camera (Hamamatsu, Japan), providing 16-bit images with 4 megapixels of resolution. The intensity extractions were performed in Zen 2 pro.

### *Fluoro-electrochemical cell and set up*

The fluoro-electrochemical thin-layer cell, shown schematically in SI Figure 1, consists of three electrodes with two carbon fibre wires (diameter  $7\mu\text{m}$ , Goodfellow Cambridge Ltd.) which act as working and counter electrodes, and a silver epoxy coated carbon fibre wire function as a pseudo-reference electrode. The cell depth is roughly  $50\mu\text{m}$ . Potentiostatic control and synchronization with the camera was provided by a previously developed in-house built device<sup>6</sup> and current-amplifier (Keithley 427) from Keithley Instruments Inc, US.



SI figure 1. Schematic of the thin-layer fluoro-electrochemical cell.

## Section 3: Videos of the fluoro-electrochemical experiments

Uploaded with the main SI are three microscope videos of the phytoplankton in the thin-layer electrochemical cell. The video descriptions are given below:

### Video 1 (1\_H\_coffeaeformis.mp4)

This video depicts the oxidative response of the diatom *H.coffeaeformis* to a potential step of +2.3 V. The video has been taken under epi-fluorescent illumination; hence the diatoms appear as bright spots in the optical field. The position of the working electrode is schematically indicated on the video. The video is displayed at 5 times faster than real-time.

### Video 2 (2\_Three\_Species.mp4)

This video depicts the electrochemical response of three different phytoplankton species in a thin-layer electrochemical cell again under epi-fluorescent illumination. These three species were selected for their ease of identification under the microscope as demonstrated in the video.

The video is displayed at 3 times faster than real-time.

### Video 3 (3\_S\_trochoidea.mp4)

This video depicts the oxidative response of a dinoflagellate (*S. trochoidea*) and a diatom (*H. coffeaeformis*) towards a strongly oxidising potential of +2.3V. In this video both epi-fluorescent illumination and a low level of transmitted light has been used. The footage was also taken using a higher (x40) magnification oil immersion objective. Hence, in this video the electrode appears as a dark band across the top of the image. The larger size of the dinoflagellate and the use of the transmitted light allows the phytoplankton internal structure to be observed whilst simultaneously allowing the change in plankton fluorescence response to be monitored.

The video is displayed at 3 times faster than real-time.

## Section 4: Effect of Oxidative Potential on Phytoplankton Fluorescence

As discussed in the main text, the epi-fluorescent light source is turned on at 0 seconds and then after sixty seconds a strong oxidising potential is applied to the working electrode. The data in the main text focuses on the change in plankton fluorescence after the oxidising potential has been applied at 60 s. In the Figures shown the plankton fluorescence is normalised against its intensity as measured when the epi-fluorescent light is turned on at 0 s.

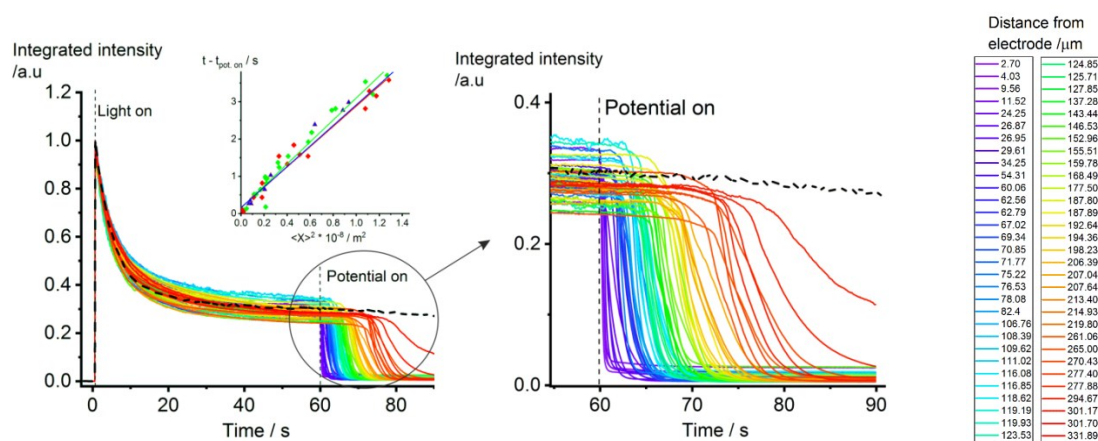
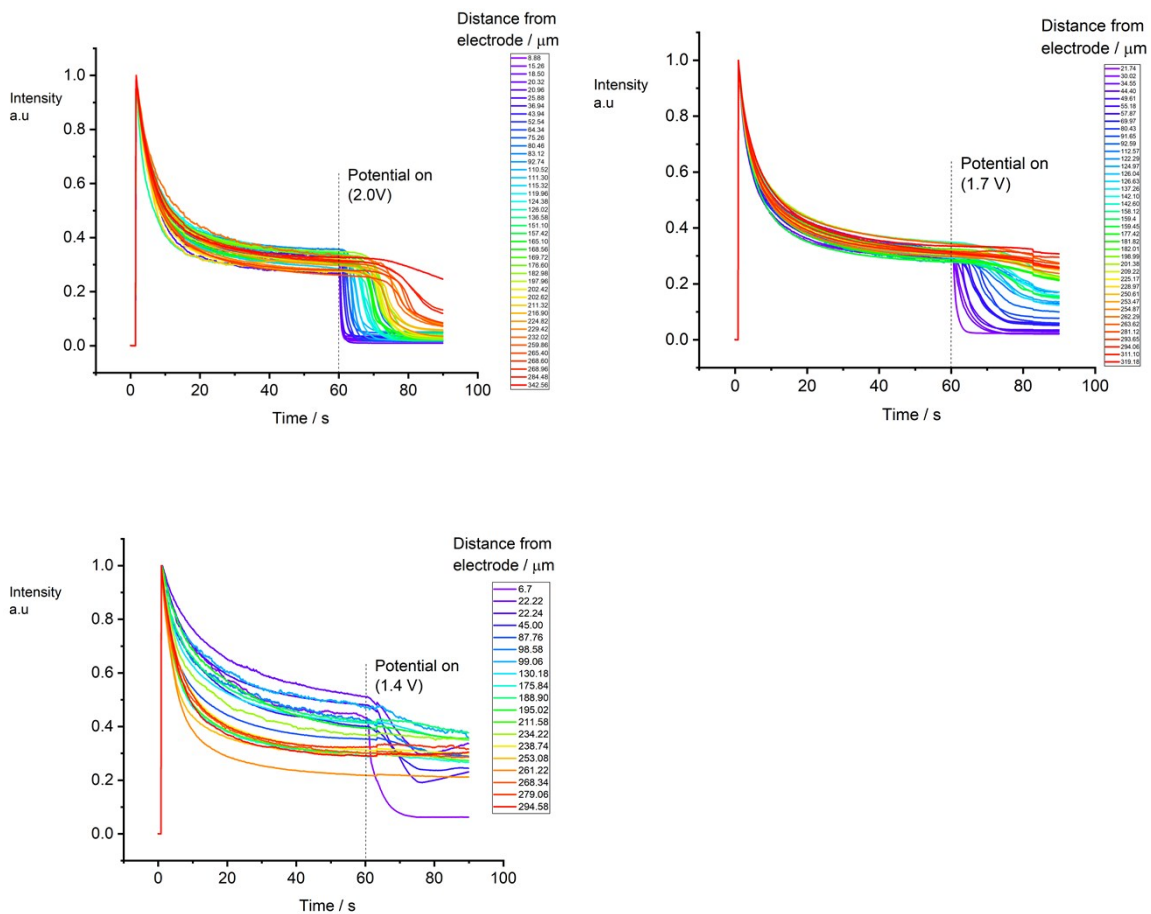


Figure 2 a) Normalised fluorescence intensity of individual *H. coffeaeformis* (diatom, CCAP 1001/2) located at different distances from the electrode during the fluoro-chronoamperometry experiment. A potential of 0.0 V (vs pseudo Ag wire) was applied from  $t = 0 - 60$  s, before the potential steps to 2.3 V for  $t = 60 - 90$  s. The colour transient from purple to blue, green, orange and red illustrates the perpendicular distance of the corresponding diatom from the electrode ranging from  $2\mu\text{m}$  to  $330\mu\text{m}$ , see SI section 5 for the colour code to distance. The black dotted line is the fluorescence decay of *H. coffeaeformis* in the absence of applied potential. Inlay shows a plot of the time taken for a diatom's fluorescence intensity to drop abnormally due to the potential step, versus the measured perpendicular distance of the diatoms from the electrode, squared.

SI Figure 2 demonstrates that after the epi-fluorescent light is turned on there is an initial rapid decrease in the fluorescence intensity of the diatoms. Figure 2 of the main text is a subset of the data shown in SI Figure 2, where in the main text the intensity is normalised against the value at 60s (i.e. when the potential is applied to the electrode). After 40 seconds of illumination the diatom fluorescence intensity decreases to approximately 35% of its original value. Note this initial decrease in the fluorescence intensity is not related to the occurrence of any reaction at the electrode surface but is due to the high light intensity used as part of the epi-fluorescent microscope setup. This

decrease is well known<sup>7</sup> and is associated with the plankton protecting themselves from photochemically induced cellular damage.<sup>8</sup> The black dotted line overlaid in SI Figure 2 shows the measured fluorescence response of a *H. coffeaeformis* diatom where an oxidising potential has **not** been applied at 60 seconds. Here it is clear; although the fluorescence intensity decreases over the course of 90 seconds, the fluorescence intensity is relatively invariant after 40 seconds of light.

SI Figure 3 shows three plots of the intensity time transient but with a less oxidative potential applied to the electrode; namely 2.0, 1.7 and 1.4V (vs saturated calomel electrode). The fluorescence intensity transients with an applied potential of 2.0V are comparable to those recorded at 2.3V; over the course of the experiments the fluorescence intensity of the diatoms within 300 $\mu$ m of the electrode were affected by applied potential. At a lower oxidative potential, however, the rate of fluorescence switch off decreases and the diatoms further away from the electrode are not significantly affected. For potential step of 1.4V, only the diatoms within  $\sim$ 60 $\mu$ m of the electrode are significantly affected by the electrochemically generated species. As mentioned in the main text, a potential of  $\sim$ 1.9V (vs SCE) is on the basis of the Nernst equation required for a favourable formation of millimolar concentration of hydroxyl radicals. Thus the observations at lower applied potentials are the result of insignificant electrochemical driving force for radical production. Moreover, the fluorescence of the phytoplankton were not affected by reductive potentials as negative as -2.0V.



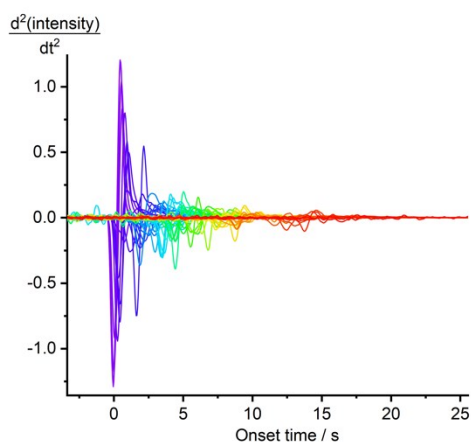
SI Figure 3. The fluorescence intensity of diatom in the fluoro-electrochemical experiment. An applied potential of 0V was applied for 0-60s. At t = 60, the potential is step from 0V to an oxidative potential of : plot a) 2.0V, plot b) 1.7V and plot c) 1.4V. The legend of each plot shows the individual colour plotted for the diatom distance from the electrode.



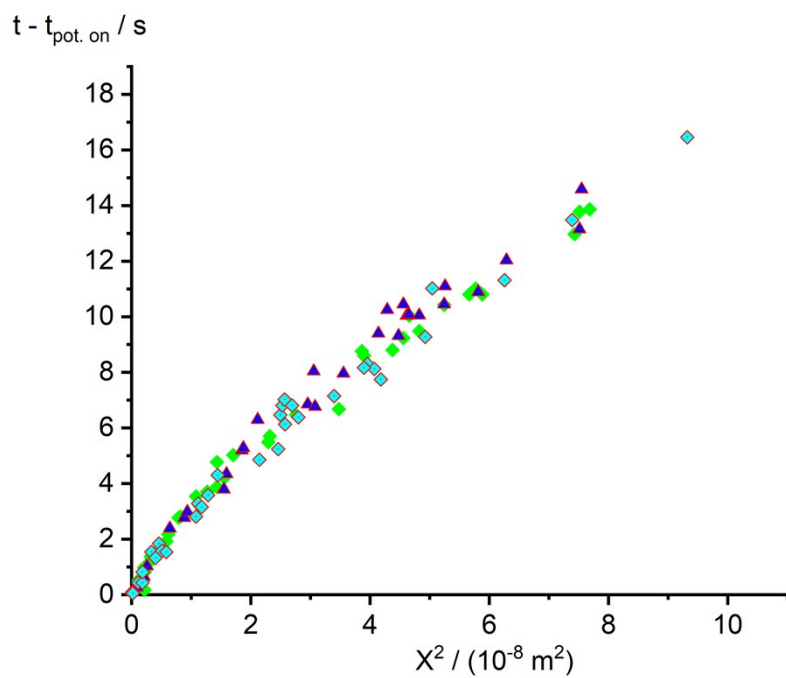
## Section 5: Data analysis

The fluorescence intensity time transients of the phytoplankton (as depicted in SI Fig.2) measured in the fluoro-electrochemical experiment were analysed using the second derivative of intensity (with respect to time) to obtain the “onset time” after which the phytoplankton fluorescence were affected upon applied of the electrode potential. The black dotted line in SI Fig.2 shows the natural fluorescence decay of the diatom upon the light on - this decay is known to be associated with the self-protection mechanism of the chlorophyll-a containing photosystem II to prevent photochemical induced cellular damage. For the first 60s, the fluorescence light is switched on and the fluorescence intensity approaches a near steady state. At  $t = 60s$ , or onset time of 0, the electrode potential steps to +2.3V. To obtain an estimate for time at which the electrode potential starts to influence the phytoplankton fluorescence intensity, the second order derivative of the intensity with respect to time are calculated and plotted in SI Figure 4. The minimum of the second derivatives correspond to the point of *greatest change* of the gradient of intensity with time and were used to determine the onset time for the fluorescence decrease.

SI Figure 5 shows a plot of onset time of fluorescence response verses the distance from the wire squared. At short times a linear relationship can be seen. However, at longer times, a deviation from the initial gradient is seen (see SI section 8 for future explanation).



SI Figure 4. A plot of the second derivative of Fig.2 versus onset time of potential step. A Savitzky–Golay filter with 2<sup>nd</sup> order of polynomial fitting and 20 points of window were used to calculate the second derivative.

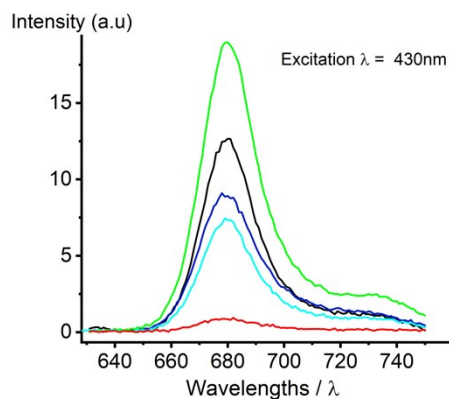


SI Figure 5, plot of time taken for the diatoms to respond to the applied potential of +2.3V (vs pseudo Ag wire) versus the corresponding diatom's perpendicular distance away from the electrode square, repeated over three experiments

## Section 6: Chemical Effects on Phytoplankton Fluorescence

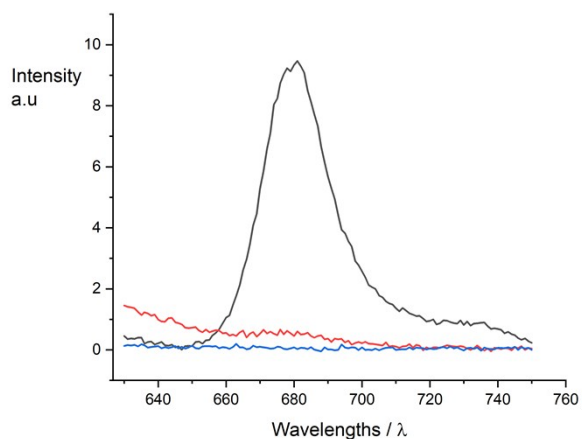
In this work the fluorescence response of different phytoplankton species were studied with an applied potential of +2.3V (vs Ag) on a carbon fibre electrode. The f/2 culture medium which the diatom were cultured in contains large amount of salt – predominantly sodium chloride. At this oxidising potential, the generation of the following species are thermodynamically favourable: chlorine from oxidation of  $\text{Cl}^-$  anion, and oxygen, <sup>9-12</sup> hydrogen peroxide and hydroxyl radicals from hydrolysis of water. However, due to the lack of adsorption sites for the stabilisation of intermediates on carbon surface (in contrast with platinum surfaces for example) will likely lead to the formation of hydroxyl radicals and hydrogen peroxide from the hydrolysis of water. Likewise the formation of  $\text{Cl}_2$  primary via a  $\text{Cl}$  intermediate is less favourable on the carbon surface as compared to a platinum surface. The following section studies the effects of the above-mentioned chemical species on the fluorescence of phytoplankton (*H. coffeaeformis*).

SI Figure 6 shows the fluorescence spectrometer measurements of the *H. coffeaeformis* culture with the addition of different chemicals. Most notably, the addition of protons (0.1M HCl),  $\text{H}_2\text{O}_2$  (33%) and  $\text{Fe}^{2+}$  (0.1M  $\text{FeSO}_4$ ) separately does not detrimentally effect the chlorophyll-a emission at 680nm. The minor variations in fluorescence intensity between experiments, most likely reflects the sedimentation of diatom and the self-protection mechanism to strong incident light. However, the addition of both  $\text{Fe}^{2+}$  (0.1M) and  $\text{H}_2\text{O}_2$  (33%), known as “Fenton’s reagent” which in situ generates  $\text{OH}\cdot$  (Eq.2 and 3 main article), dramatically kills the phytoplankton fluorescence.

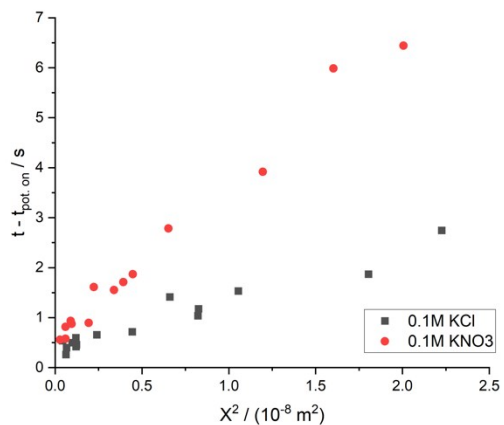


SI Figure 6. Fluorescence spectrometer emission measurements of 2.5ml *H. coffeaeformis* culture with the addition of 0.5ml of: black line – H<sub>2</sub>O, blue line - 0.1M HCl, green line – 33% H<sub>2</sub>O<sub>2</sub>, turquoise line – 0.1M FeSO<sub>4</sub> and red line – 0.1M FeSO<sub>4</sub> and 33% H<sub>2</sub>O<sub>2</sub> (Fenton's reagent).

SI Figure 7 shows the fluorescence spectrometer measurements of the *H. coffeaeformis* culture with the addition of NaOCl or chlorine gas. The results shows a strong fluorescence effect in the present of Cl<sub>2</sub> (and NaOCl) similar to that observed with Fenton's reagent. Moreover, SI Figure 8 shows a plot of the fluorescence response time of individual diatoms to the applied potential, verses distance squared, in chloride containing medium and non-chloride containing medium. At similar distances away from the electrode, the presence of Cl<sup>-</sup> anion in the solution leads to a faster fluorescence switch off compare to NO<sub>3</sub><sup>-</sup>. This shows that fluorescence susceptibility of *H. coffeaeformis* to the electrode generated species is higher in the chloride containing medium, which may be due to the formation of chlorine gas. However, as evidenced by SI figure 8 where the electrochemical inhibition occurs in 0.1 M KNO<sub>3</sub>, chloride is not essential for the fluorescence switch off.



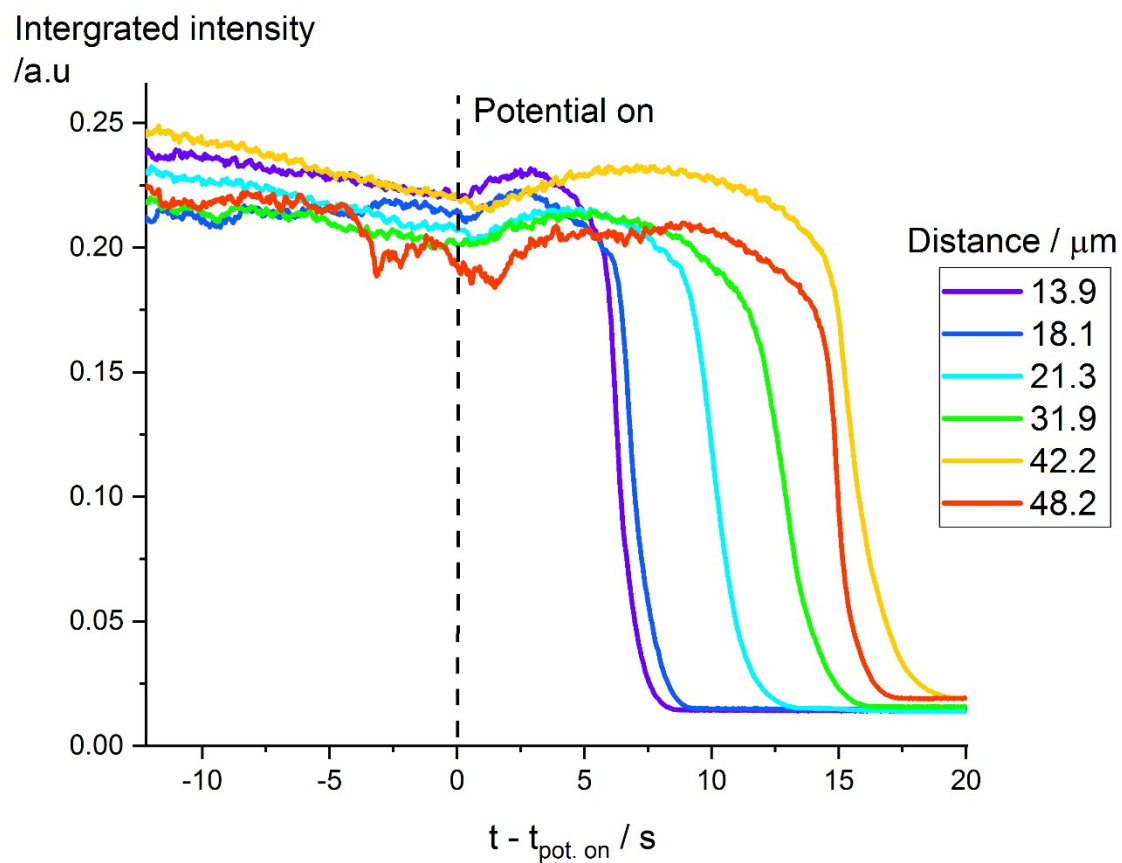
SI Figure 7. Fluorescence spectrometer emission measurements of 2.5ml *H.coffeaeformis* culture with the addition of 0.5ml of: black line – H<sub>2</sub>O, red line – NaOCl (1.26g/ml) and blue line – H<sub>2</sub>O + chlorine gas.



SI Figure 8. The offset time which the fluorescence of individual *H.coffeaeformis* responses to the onset potential of +2.3V (vs Ag) plotted against their distance away from the electrode squared. The *H.coffeaeformis* culture were centrifuged for 1 min at 1000 rpm and the supernatant were replaced with 0.1M KNO<sub>3</sub> (red circles) or 0.1M KCl (black squares).

## Section 7: Fluorescence response of *E. huxleyi*

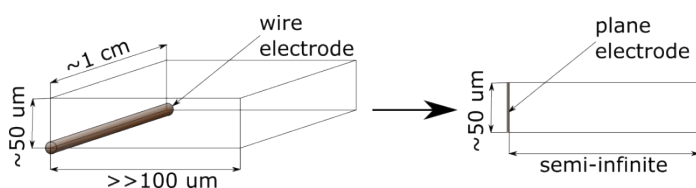
Figure 3 in the main text shows a representative intensity profile of a *H. coffeaeformis* and *E. huxleyi* in the same experiment (video two) and at equal distance from the electrode ( $\sim 20 \mu\text{m}$ ). The fluorescence responses of the two species are distinctively different; the intensity of the *H. coffeaeformis* plummets within seconds after application of a high oxidising potential. In contrast *E. huxleyi* shows a slight rise in intensity before the fluorescence falls after  $\sim 14$  seconds. SI Figure 9 shows the fluorescence responses of a sample of *E. huxleyi* in presented in Video Two – all show a small rise in fluorescence intensity before rapidly switching off. This rapid decrease in intensity indicates that the plankton outer structure is not initially permeable to the formed radicals but the once that cell wall or membrane has been breached the cell rapidly loses its fluorescence signal. Note if the different behaviour was due to slow mass-transport through the cells internal structure or due to low permeability of the radical species across the interface one would expect the intensity/time transients to be markedly different - in this case one would expect a slower and monotonic decrease in the phytoplankton fluorescence response. The results in SI Figure 9 indicate that the microalgal cell wall or membrane is chemically attacked by the formed radical species leading to a catastrophic and rapid loss of integrity.



SI Figure 9. Normalised fluorescence intensity of individual *E. Huxleyi* located at different distances from the electrode during the fluoro-chronoamperometry experiment (as shown in Video Two). At time of 60 seconds a potential of +2.3V (vs Ag pseudo wire) is applied to the electrode.

## Section 8: Analytical Model for the Phytoplankton Fluorescence Response

In this section we seek to provide a simplified model of the phytoplankton response towards the production of radicals at the electrochemical interface. Specifically, we wish to provide insight into the physical factors controlling the ‘switching-off’ of the plankton fluorescence as a function of time and distance to the electrode surface (as quantified in Figure 4a of the main text). Due to the necessary requirement of the reactive species diffusing away from the electrode surface before they can react with and induce damage to the phytoplankton, the resulting measured fluorescence response arises from a convolution of multiple physical and chemical factors.



SI Figure 10: Geometry of the actual cell and that used in the presented diffusional model. The electrochemical microscope cell contains a carbon fibre working electrode (radius  $3.5 \mu\text{m}$ , length  $\sim 1 \text{ cm}$ ), in a thin-layer cell of  $50 \mu\text{m}$  in height and with a width of far greater than  $100 \mu\text{m}$ . Note in the present work only the fluorescence response of plankton within approximately  $100 \mu\text{m}$  of the wire electrode are monitored and analysed. In order to simplify the analysis the cell geometry is simplified to that of a one-dimensional problem.

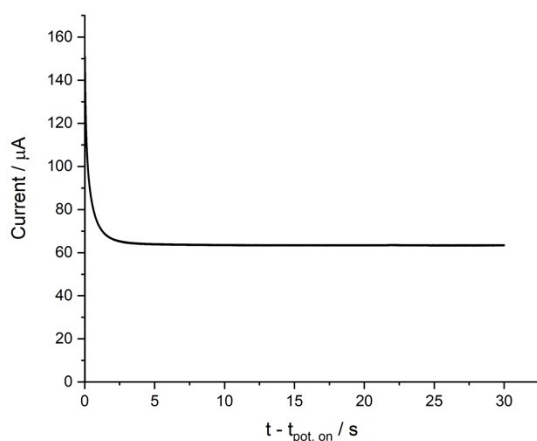
Here, to provide a readily approachable model for this problem, it is assumed that the solution phase radical concentration must reach a threshold ( $C_{\text{thres}}$ ) value, possibly required for the initial destruction of the cell wall, prior to inducing the oxidative destruction of the phytoplankton fluorescence response. Moreover, as depicted in SI Figure 1 the geometry of the cell can be simplified to become a one dimensional problem.

In one dimension and in accordance with the Cottrell equation the electrochemical flux ( $j / \text{mol m}^{-2} \text{ s}^{-1}$ ) at the electrode interface can be described by:

$$j_{elec} = C_0 \left( \frac{D}{\pi t} \right)^{0.5} \quad (1)$$



where  $C_0$  is the concentration at the electrode interface,  $D$  is the diffusion coefficient of the electroactive species ( $\text{m}^2 \text{s}^{-1}$ ) and  $t$  is the experimental time (s). Given that in the experiment the solvent is the electro-active reagent and that only a small fraction of the interfacial water is oxidised then, during the course of the chronoamperogram, the electrochemical ( $j_{elec}$ ) flux will be relatively constant as a function of time. At +2.3 V vs Ag the recorded total current at the electrode was found to be  $\sim 60 \mu\text{A}$ ; an example experimental chronoamperogram is depicted in SI Figure 11 showing the steady-state nature of the current. In this section and as depicted in SI Figure 10, this model assumes that this current is produced at an electrode of dimensions  $0.01 \times 50 \times 10^{-6} \text{m}^2$ . Hence, this gives an average electrochemical flux of approximately  $1 \times 10^{-3} \text{mol m}^{-2} \text{s}^{-1}$ .



SI Figure 11. Current-time transient during a typical fluoro-electrochemical chronoamperometry experiment. At  $t - t_{pot, on} = 0$ , the potential is stepped to +2.3V vs Ag. Where  $t_{pot, on}$  is the time at which electrode potential is stepped to +2.3V.

In the timeframe of the experiment the biologically dominant chemical species are the oxidative radicals produced by the electrochemical reaction. It is likely that only a small fraction of the current will lead to the production of radical species, such that the flux of radicals ( $j_{rad}$ ) will be less than the electrochemical flux ( $j_{elec}$ ). This may be expressed in a simple manner through accounting for the Faradaic efficiency ( $E_{ff}$ ) of the interfacial reaction ( $j_{rad} = E_{ff} j_{elec}$ ). In the following we assume an arbitrary efficiency of 1%. Hence, the interfacial radical flux ( $j_{rad}$ ) is taken as a constant and given a value of  $1 \times 10^{-5} \text{mol m}^{-2} \text{s}^{-1}$ . Using SI equation 1 and on the above argument setting the interfacial

radical flux as a constant, the concentration of radicals ( $C_{rad,x=0}$ ) at the interface can be approximately expressed as:

$$C_{rad,x=0} = j_{rad} \left( \frac{\pi t}{D} \right)^{0.5} \quad (2)$$

This equation defines that under these constant electrochemical flux conditions the surface concentration of the radicals will approximately increase with the square-root of time.

In one dimension the concentration profile ( $C(x,t)$ ) away from the electrochemical interface is:

$$C_{rad}(x,t) = C_{rad,x=0} \operatorname{erfc} \left( \frac{x}{2\sqrt{Dt}} \right) \quad (3)$$

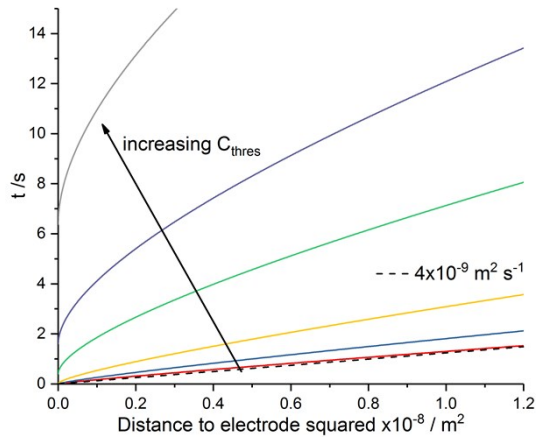
where  $\operatorname{erfc}$  is the complementary error function. Consequently, substitution of SI Equation 2 into SI Equation 3, and setting  $C(x,t)$  equal to some threshold concentration value gives the following:

$$x = 2\sqrt{Dt} \operatorname{erfc}^{-1} \left( \frac{C_{thres} (D)}{j_{rad} (\pi t)^{0.5}} \right) \quad (4)$$

where  $\operatorname{erfc}^{-1}$  is the inverse complementary error function; the function here only yields physically relevant values when the input lies between 0 and 1. SI Equation 4 is an approximate analytical expression that describes how the distance at which the plankton fluorescence 'switches-off' varies as a function of: the experimental time, the radical diffusion coefficient, the flux of radical production at the electrode surface and the sensitivity of the plankton towards the radicals (as expressed through the value of  $C_{thres}$ ).

To facilitate direct comparison of the above SI Equation 4 to the experimental results of different phytoplankton species as presented in Figure 4a of the main article, SI Figure 12 plots the results of SI equation 4 with differ values of  $C_{thres}$  ( $5 \times 10^{-4}$  to 0.2 mM) as the distance squared against the time. Here we have taken a representative diffusion coefficient of  $5 \times 10^{-10} \text{ m}^2 \text{ s}^{-1}$  for the aqueous based species and have used the likely physically realistic radical flux ( $j_{rad}$ ) of  $1 \times 10^{-5} \text{ mol m}^{-2} \text{ s}^{-1}$ . Also

plotted is a reference line (dashed) of the equation  $\langle x \rangle^2 = 2Dt$  where  $D$  has been given a value of  $4 \times 10^{-9} \text{ m}^2 \text{ s}^{-1}$ , which is to be contrasted with the analytical result as discussed (varying  $C_{\text{thres}}$  with  $D = 5 \times 10^{-10} \text{ m}^2 \text{ s}^{-1}$ ).



SI Figure 12: The predicted plankton fluorescence 'switch-off' time as a function of the distance from the electrode surface, as given by the approximate analytical SI equation 4.  $D_{\text{rad}} = 5 \times 10^{-10} \text{ m}^2 \text{ s}^{-1}$ ,  $j_{\text{rad}} = 1 \times 10^{-5} \text{ mol m}^{-2} \text{ s}^{-1}$ ,  $C_{\text{thres}} = 5 \times 10^{-4} \text{ mM}$  (red),  $0.002 \text{ mM}$  (blue),  $0.01 \text{ mM}$  (yellow),  $0.05 \text{ mM}$  (green),  $0.1 \text{ mM}$  (purple) and  $0.2 \text{ mM}$  (grey). Also overlaid for comparison with a dashed line is the expression  $t = x^2/2D_{\text{eff}}$ , where here effective diffusion coefficient ( $D_{\text{eff}}$ ) has been given a value of  $4 \times 10^{-9} \text{ m}^2 \text{ s}^{-1}$ .

SI Figure 12 presents a number of important features. First, the value of  $C_{\text{thres}}$  partially controls the time at which the phytoplankton fluorescence responds to the electro-generated oxidative species; for a given electrode radical flux higher values of  $C_{\text{thres}}$  increases the time required – at a given distance from the electrode – for the fluorescence to be affected. Second, a non-zero intercept is predicted at high threshold values. Third, in the long time limit or for low threshold values the plot becomes quasi-linear. This quasi-linearity arises for small values of the input of the  $\text{erfc}^{-1}$  function. Although  $\text{erfc}^{-1}$  tends to infinity at zero it does so very slowly, consequently for reasonable values of the input value to the  $\text{erfc}^{-1}$  function it has an approximate limit of  $\sim 2$ . Consequently, in this low  $C_{\text{thres}}$  or long time limit SI equation 4 becomes approximately equal to  $x = 4\sqrt{Dt}$  ( $t = x^2/16D$ ), where in this analysis the value of  $D$  has been taken as  $5 \times 10^{-9} \text{ m}^2 \text{ s}^{-1}$ . Hence, for the  $C_{\text{thres}}$  value of  $5 \times 10^{-4} \text{ mM}$ , as plotted in SI figure 12, SI equation 4 is approximately equal to the equation  $t = x^2/2D_{\text{eff}}$ , where the effective diffusion coefficient has a value of  $4 \times 10^{-9} \text{ m}^2 \text{ s}^{-1}$ , this is plotted as the dashed line on SI Figure 12. Fourth, As the concentration threshold is increased the output of the  $\text{erfc}^{-1}$  function

decreases leading to a change in the gradient of the plot, the curvature present for the high  $c_{\text{thres}}$  values (0.2 mM for example) reflects, in this limit, the variability of the  $\text{erfc}^{-1}$  function with time.

In this main text of this work the gradient of the plot of the fluorescence 'switch-off' time against the distance the phytoplankton is away from is used as a measure of the microalgal sensitivity towards oxidative radical damage. The gradient is reported as a *susceptibility factor*, as related to the inverse gradient of a plot of time vs distance squared. This analysis shows that this "effective" diffusion coefficient represents the mass-transport of the radical species multiplied by some unknown but species specific 'phytoplankton' sensitivity factor towards the generated radical. As demonstrated above this effective diffusion coefficient can be larger than the actual diffusion coefficient of the molecular (radical) species. The measured effective diffusion coefficient will also be sensitive to the magnitude of the experimentally used oxidative flux ( $j_{\text{rad}}$ ). High values of the measured susceptibility factor indicate a relative high sensitivity or vulnerability of the plankton towards oxidative radical attack; conversely, lower values indicate increased plankton resilience. Given in this work the chemical conditions are the same throughout the work such that the radical diffusion coefficient and electrode flux are essentially constants then the measured susceptibility factor for the different phytoplankton can be used a direct comparator of the different species sensitivity towards oxidative radical attack.

## References

1. R. E. Hecky, K. Mopper, P. Kilham and E. T. Degens, *Mar. Biol.*, 1973, **19**, 323-331.
2. J. G. Stepanek and J. P. Kociolek, *Protist*, 2014, **165**, 177-195.
3. J. C. Green, P. A. Course and G. A. Tarran, *J. Mar. Syst.*, 1996, **9**, 33-44.
4. D. Klaveness and E. Paasche, *Arch. Microbiol.*, 1971, **75**, 382-385.
5. F. M. M. Morel, J. G. Rueter, D. M. Anderson and R. R. L. Guillard, *J. Phycol.*, 1979, **15**, 135-141.
6. C. Batchelor-McAuley, J. Ellison, K. Tschulik, P. L. Hurst, R. Boldt and R. G. Compton, *Analyst*, 2015, **140**, 5048-5054.
7. D. Lazár, *Biochim. Biophys. Acta Bioenerg.*, 1999, **1412**, 1-28.
8. N. E. Holt, D. Zigmantas, L. Valkunas, X.-P. Li, K. K. Niyogi and G. R. Fleming, *Science*, 2005, **307**, 433-436.
9. J. Jordan, E. Ackerman and R. L. Berger, *J. Am. Chem. Soc.*, 1956, **78**, 2979-2983.
10. R. E. Davis, G. L. Horvath and C. W. Tobias, *Electrochim. Acta*, 1967, **12**, 287-297.
11. D. M. Himmelblau, *Chem. Rev.*, 1964, **64**, 527-550.
12. S. A. M. van Stroe-Biezen, F. M. Everaerts, L. J. J. Janssen and R. A. Tacke, *Anal. Chim. Acta*, 1993, **273**, 553-560.